

Turtle–Chicken Chimera: An Experimental Approach to Understanding Evolutionary Innovation in the Turtle

Hiroshi Nagashima,^{1,2} Katsuhisa Uchida,^{1†} Keiko Yamamoto,¹ Shigehiro Kuraku,¹ Ryo Usuda,¹ and Shigeru Kuratani^{1*}

Turtles have a body plan unique among vertebrates in that their ribs have shifted topographically to a superficial layer of the body and the trunk muscles are greatly reduced. Identifying the developmental factors that cause this pattern would further our understanding of the evolutionary origin of the turtles. As the first step in addressing this question, we replaced newly developed epithelial somites of the chicken at the thoracic level with those of the Chinese soft-shelled turtle *Pelodiscus sinensis* (*P. sinensis* somites into a chicken host) and observed the developmental patterning of the grafted somites in the chimera. The *P. sinensis* somites differentiated normally in the chicken embryonic environment into sclerotomes and dermomyotomes, and the myotomes differentiated further into the epaxial and hypaxial muscles with histological morphology similar to that of normal *P. sinensis* embryos and not to that of the chicken. Epaxial dermis also arose from the graft. Skeletal components, however, did not differentiate from the *P. sinensis* sclerotome, except for small fragments of cartilage associated with the host centrum and neural arches. We conclude that chicken and *P. sinensis* share the developmental programs necessary for the early differentiation of somites and that turtle-specific traits in muscle patterning arise mainly through a cell-autonomous developmental process in the somites per se. However, the mechanism for turtle-specific cartilage patterning, including that of the ribs, is not supported by the chicken embryonic environment. *Developmental Dynamics* 232:149–161, 2005. © 2004 Wiley-Liss, Inc.

Key words: somites; ribs; transplantation; turtles; evolutionary innovation

Received 20 July 2004; Revised 7 September 2004; Accepted 7 September 2004

INTRODUCTION

The turtle shell is often cited as a typical example of evolutionary novelty because of its unusual anatomical composition; the dorsal half of the shell, or the carapace, is based on ribs that have moved to a superficial position, covering the limb girdles dorsally (reviewed by Hall, 1998; Gilbert et al., 2001; Rieppel, 2001). These changes

in the topographical relationships of the skeletal elements, which also correlate with morphological changes in the muscles, appear to be due to the lateral growth of the ribs and not to the descent of the girdles into the rib cage (Ruckes, 1929; Walker, 1947; Emelianov, 1936; reviewed by Burke, 1989, 1991; Ewert, 1985). This shift in rib growth also appears to be the basis

of modified tissue interactions that yield the dermal bones and expanded scales of the carapace (reviewed by Hall, 1998). A small change in the place of development (heterotopy; Haeckel, 1875) can result in a large-scale alteration in morphology. The function of carapacial ridge (CR) has been assumed (Burke, 1989) in the topographical shift of the ribs. The CR is

¹Laboratory for Evolutionary Morphology, Center for Developmental Biology (CDB), RIKEN Kobe, Kobe, Japan

²Graduate School of Science and Technology, Kobe University, Kobe, Japan

Grant sponsor: the Ministry of Education, Science, and Culture of Japan.

[†]Dr. Uchida's present address is Sado Marine Biological Station, Faculty of Science, Niigata University, 87 Tassha, Sado, Niigata 952-2135, Japan.

*Correspondence to: Shigeru Kuratani, Laboratory for Evolutionary Morphology, Center for Developmental Biology (CDB), RIKEN, 2-2-3 Minatojima-minami, Chuo-ku, Kobe, Hyogo 650-0047, Japan. E-mail: saizo@cdb.riken.jp

DOI 10.1002/dvdy.20235

Published online 3 December 2004 in Wiley InterScience (www.interscience.wiley.com).

a structure that consists of aggregated mesenchyme surrounded by thickened ectoderm and appears in the flank of the late pharyngula. By surgical removal of the CR, Burke (1991) showed that the CR is required for normal rib growth of the turtle. Thus, an inductive activity similar to that in the limb bud, has been assumed in the CR (Burke, 1989, 1991), and in the same context, CR-specific localization of some molecules and gene expressions have been reported recently (Burke, 1989; Loredó et al., 2001; Vincent, 2003).

In association with shell formation, the trunk muscles (both epaxial and hypaxial muscles) of turtles are greatly reduced at the flank level. Importantly, both the trunk muscles and the ribs differentiate from somites, the segmented mesodermal blocks in the early embryo (Seno, 1961; Pinot, 1969; Sweeney and Watterson, 1969; Christ et al., 1974; Christ and Wilting, 1992; Huang et al., 1994, 1996, 2000; Kato and Aoyama, 1998; Evans, 2003). From the perspective of evolutionary developmental biology, therefore, the key to innovation in the evolution of the turtles is the changes introduced into the developmental programs of the somite derivatives.

As for turtle somite development, Yntema (1970) showed in *Chelydra serpentina* that removal of somites leads to the loss of scutes and ribs in the carapace. He also thought that the turtle ribs are derived from the lateral part of the somites. The developmental fates and mechanisms of differentiation of amniote somites have been studied more extensively in model animals such as the chicken and mouse (reviewed by Christ and Ordahl, 1995; Christ et al., 2000; Dockter, 2000; Monsoro-Burq and Le Douarin, 2000; Brent and Tabin, 2002). Newly segmented epithelial somites undergo initial differentiation into the ventromedial deepithelialized part, or the sclerotome, and the rest of the somite, generally called the dermomyotome (Christ and Ordahl, 1995; Christ et al., 2000). The sclerotome then gives rise to skeletal elements, including the vertebrae and ribs during later development (Christ and Wilting, 1992; Huang et al., 1994, 1996; Evans, 2003). It has also been suggested that at least a part of the rib differentiates

from the dermomyotome (Kato and Aoyama, 1998). In the developmental patterning of turtle somites, the most intriguing questions are: What changes have been introduced during the evolution of this animal group? Into which stage of its development were they introduced, relative to the generalized time table of somite development in amniotes such as the chicken and mouse?

The turtle-specific traits of somite differentiation and the developmental mechanisms responsible for these traits should reflect the functions of the alleles actually selected during the evolutionary establishment of the turtles. Importantly, such changes would not necessarily be found in the cell-autonomous mechanism of the somite itself, because the embryonic environment surrounding the somites can also exert various signals through tissue interactions that determine the specific developmental fates of somite-derived cells. Therefore, the turtle-specific developmental program can be classified into the cell-autonomous and non-cell-autonomous (or epigenetic) factors involved in somite differentiation.

In the present study, as a first step in determining the cell-autonomous factors involved in turtle-specific patterning mechanisms, interspecies chimeras were constructed between chicken and turtle, i.e., turtle somites were transplanted into chicken hosts at comparable developmental stages (Fig. 1). Although the phylogenetic position of the turtles remains enigmatic, recent molecular phylogenetic analyses have supported the close affinity of birds, crocodiles, and turtles (Platz and Conlon, 1997; Zardoya and Meyer, 1998, 2001a,b; Hedges and Poling, 1999; Kumazawa and Nishida, 1999; Mannen and Li, 1999; Cao et al., 2000), which justifies the use of *Gallus gallus* as a competent host for the chimera. As the donor species, we selected the Chinese soft-shelled turtle *Pelodiscus sinensis*, which is commercially available from fish farms in Japan (Fig. 1). To trace the cell lineages of *P. sinensis* graft derivatives, we raised anti-*P. sinensis* IgY, which successfully labeled *P. sinensis* cells in the unstained chicken background. Young transplanted somites from *P. sinensis* responded to the chicken em-

brionic environment, differentiating into sclerotomes and dermomyotomes. However, although the cell-autonomous nature of somite differentiation was apparent in muscle differentiation, the skeletal differentiation of *P. sinensis* somites was substantially arrested in the chimeric environment.

RESULTS

Comparative Anatomy of Embryonic Thoracic Regions and Somitic Derivatives

The morphology of the thoracic regions was compared between *P. sinensis* and *G. gallus* embryos at stages when species-specific anatomical features become apparent (Fig. 2A,B). In the chicken, myotomes differentiated into the epaxial muscle in the dorsal part of the body and into the hypaxial muscles in the lateral body wall (Fig. 2A). In the chicken-quail chimera, in which the somites of the chicken host had been unilaterally replaced by those of the quail, the somite-derived dermis was predominantly distributed in the dorsal part of the body surrounding the epaxial muscle, which was also of quail-somite origin. However, the lateral body wall did not contain dermis composed of quail cells (Fig. 2C,D), as already reported (Nowicki et al., 2003; Burke and Nowicki, 2003; Fig. 2A). Our experimental procedure for chimera construction allowed us to remove all the somitic cells from the experimental side, and half the centrum was completely replaced with quail cells (Fig. 2D). In the skeletal system, quail cells differentiated into chondroblasts of the centrum, neural arch, and ribs (Fig. 2D). Quail cells also contributed to part of the mesonephros and part of the dorsal aorta. Dorsal root ganglia were never replaced with quail cells (Fig. 2D). Therefore, in the chicken embryo, the rib primordia and hypaxial muscles derive from somites and secondarily grow ventrally into the hypaxial domain, as "primaxial" elements (Nowicki et al., 2003; Burke and Nowicki, 2003; Fig. 2A).

In the *P. sinensis* embryo, morphologically normal epaxial muscle developed, although its extent was less than that observed in the chicken host, whereas the hypaxial muscle

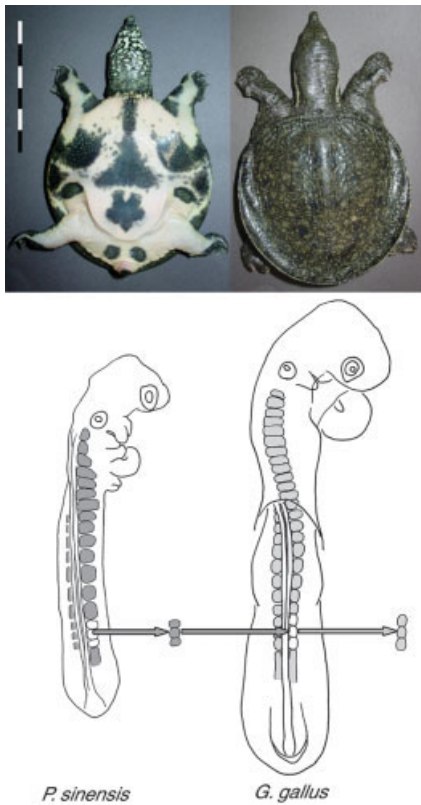


Fig. 1. *Pelodiscus sinensis* and transplantation of somites. Top: Juvenile *P. sinensis*. Below: Three successive newly formed somites (somite stages +I to +III; Ordahl et al., 1993) were removed unilaterally from the thoracic level of an Hamburger and Hamilton stage 15 chicken embryo. Three epithelial thoracic somites were excised from a Tokita and Kuratani stage 10 *P. sinensis* embryo on the corresponding side and implanted into the scar made in the host chicken embryo. Scale bar = 6 cm.

primordia appeared as a thin thread of fibrous tissue that was stained with the monoclonal antibody, MF-20 (data not shown; see below). The massive rib primordia grew more laterally compared with that of the chicken (Fig. 2A,B), and it never entered the lateral body wall; the ribs remained in the epaxial domain. Therefore, the ribs and the hypaxial muscles of *P. sinensis* did not develop side-by-side in the lateral body wall, as was seen in the chicken embryo (Fig. 2A,B). A characteristic trait of turtle embryos, the CR, grew on the lateral aspect of the body wall (Fig. 2B). This ridge was lateral to the distal tip of the rib. No such ridge appeared in the corresponding region of the chicken embryo (Fig. 2A). Because the rib never invaded the hypaxial domain but instead grew laterally toward the CR,

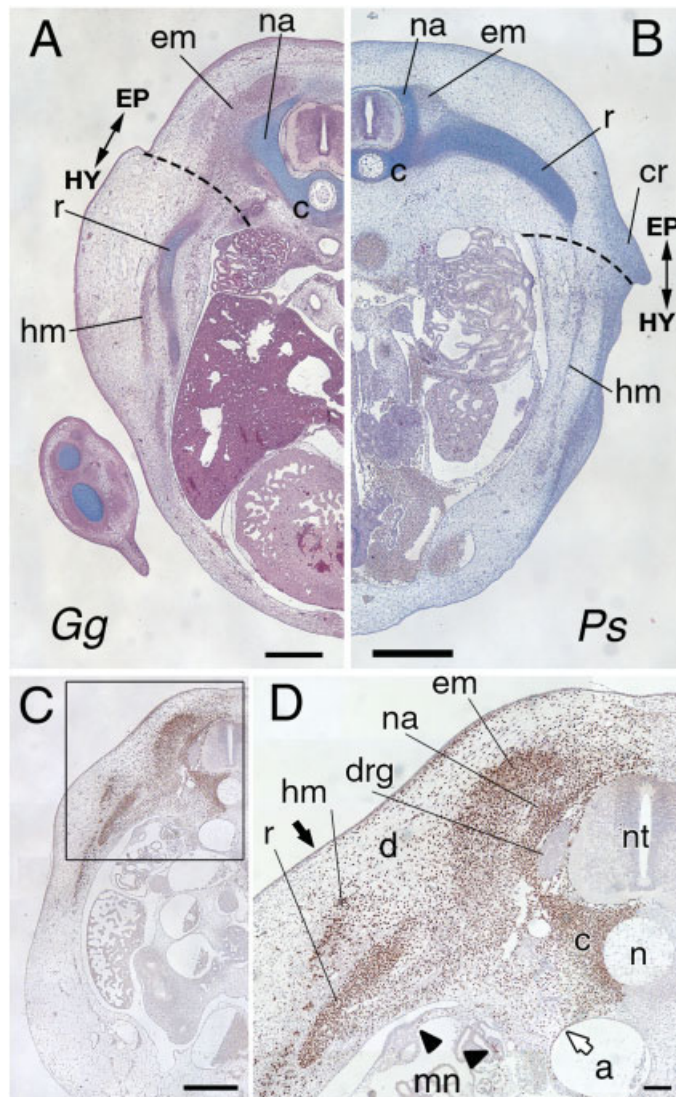


Fig. 2. Comparison of thoracic anatomy of *Gallus gallus* and *Pelodiscus sinensis* embryos. Transverse sections through the thoracic regions of *Pelodiscus* and *Gallus* stage 11 *G. gallus* (A) and *P. sinensis* (B) embryos are shown. Broken lines indicate the morphological boundaries between epaxial (EP) and hypaxial (HY) regions. **A:** In *G. gallus*, the rib (r) grows from the epaxial region ventrally into the hypaxial region, within the medial part of the somatopleure. Both the epaxial (em) and hypaxial muscles (hm) are massive. **B:** In *P. sinensis*, the rib (r) stays in the epaxial domain, growing laterally toward the carapacial ridge (cr). Epaxial (em) and hypaxial muscles (hm) are relatively smaller than those of the chicken. **C:** Transverse section of a chicken-quail chimera 4 days after surgery, in which chicken thoracic epithelial somites had been replaced with those of quail. Immunohistochemically stained with QCPN monoclonal antibody to identify quail cells and counterstained with hematoxylin. Primaxial domain of the embryonic thorax is occupied by QCPN-positive quail cells. Quail somite derivatives have moved into the lateral body wall or the hypaxial domain of the chimera. **D:** High magnification of the box in C. Arrowheads and white arrows indicate quail cells contributing to the mesonephros (mn) and the dorsal aortic wall (a), respectively. The black arrow indicates the interface between quail and chicken dermis. a, dorsal aorta; c, centrum; cr, carapacial ridge; d, dermis; drg, dorsal root ganglia; mn, mesonephros; n, notochord; na, neural arch; nt, neural tube; r, rib.

and the hypaxial muscles of *P. sinensis* always developed ventral to the distal tip of the ribs (Fig. 2B; also see Fig. 3), we can assume that the CR arises in the epaxial domain adjacent to the junction of the epaxial and hypaxial domains.

G. gallus-*P. sinensis* Common Developmental Stages

To examine the developmental pattern of *P. sinensis* somite derivatives in the chicken embryonic environ-

TABLE 1. Common Developmental Stages of *Pelodiscus sinensis* and *Gallus gallus*^a

Common stages (PG stages)	<i>P. sinensis</i> (TK stages)	<i>G. gallus</i> (HH stages)	Histological description
1	9	15	Epithelial somites.
2	10	16	Ventromedial part of somites starts to be deepithelialized to form sclerotomes.
3	11 ⁻	17	Sclerotomal cells migrate toward the notochord.
4	11	18	Initial appearance of myotomes.
5	12 ⁻	20	Formation of myotome completed; midportion of dermatome starts to be deepithelialized.
6	12	22	Ventrolateral lip of the dermomyotome invades the somatopleure.
7	12 ⁺	23	Dermatome almost deepithelialized except for its ventrolateral and dorsomedial lips.
8	13	24	Sclerotomal cells aggregate around the notochord: beginning of centrum formation. Carapacial ridge begins to appear in <i>P. sinensis</i> .
9	14 ⁻ –14	25–26	Ventrolateral lip of dermatome deepithelialized.
10	14 ⁺ –15	27–28	Appearance of rib primordia as mesenchymal condensation.
11	15 ⁺ –16	29–30	Species-specific morphology established.

^aHistological observations were made on transversely sectioned specimens at the levels of somites (s) 15–21 for *P. sinensis* and s22–26 for *G. gallus* (see Fig. 3). TK stages refer to the developmental stages of *P. sinensis* described by Tokita and Kuratani (2001), and HH stages to those described by Hamburger and Hamilton (1951) for *G. gallus* development. The common stages were established on the basis of the developmental patterning of somites. PG, *Pelodiscus* and *Gallus*.

ment, it is necessary to construct chimeras. To reduce any possible developmental arrest in the chimera that might arise from differences in developmental rates, we initially tried to establish common developmental stages at the thoracic level between the two animal species. Histological sections were examined and mesodermal development was compared in somites (s) 15–21 of *P. sinensis* and s22–26 of *G. gallus* (corresponding to the thoracic level in each species; Fig. 3). Based on this comparison, we defined common developmental stages (PG stages; PG stands for *Pelodiscus* and *Gallus*), as shown in Table 1. They ranged from the newly formed epithelial somite observed at PG stage 1, corresponding to HH stage 15 of *G. gallus* (Hamburger and Hamilton, 1951) and TK stage 9 of *P. sinensis* (Tokita and Kuratani, 2001), to PG stage 11, when the anatomical features of the muscles and skeletal elements become apparent in each species, corresponding to HH stage 30 of *G. gallus* and TK stage 16 of *P. sinensis* (Fig. 3).

Based on the above staging, developmental rates were compared at different temperatures for both species to determine the most appropriate

conditions for the incubation of chimeras (Fig. 4). *P. sinensis* developed at the greatest rate at 34°C, but the viability of embryos decreased abruptly when incubated at temperatures higher than 38°C. Although chicken embryos developed normally in the range of 34°C to 38°C, they did not develop with normal embryonic patterns at temperatures below 30°C (Fig. 4). We concluded that chimeras should be incubated most appropriately within the range of 34–36°C. Within this window, the developmental rates of both species synchronized well, especially between PG stages 1 and 5 (Fig. 4).

Anti-*P. sinensis* Antiserum

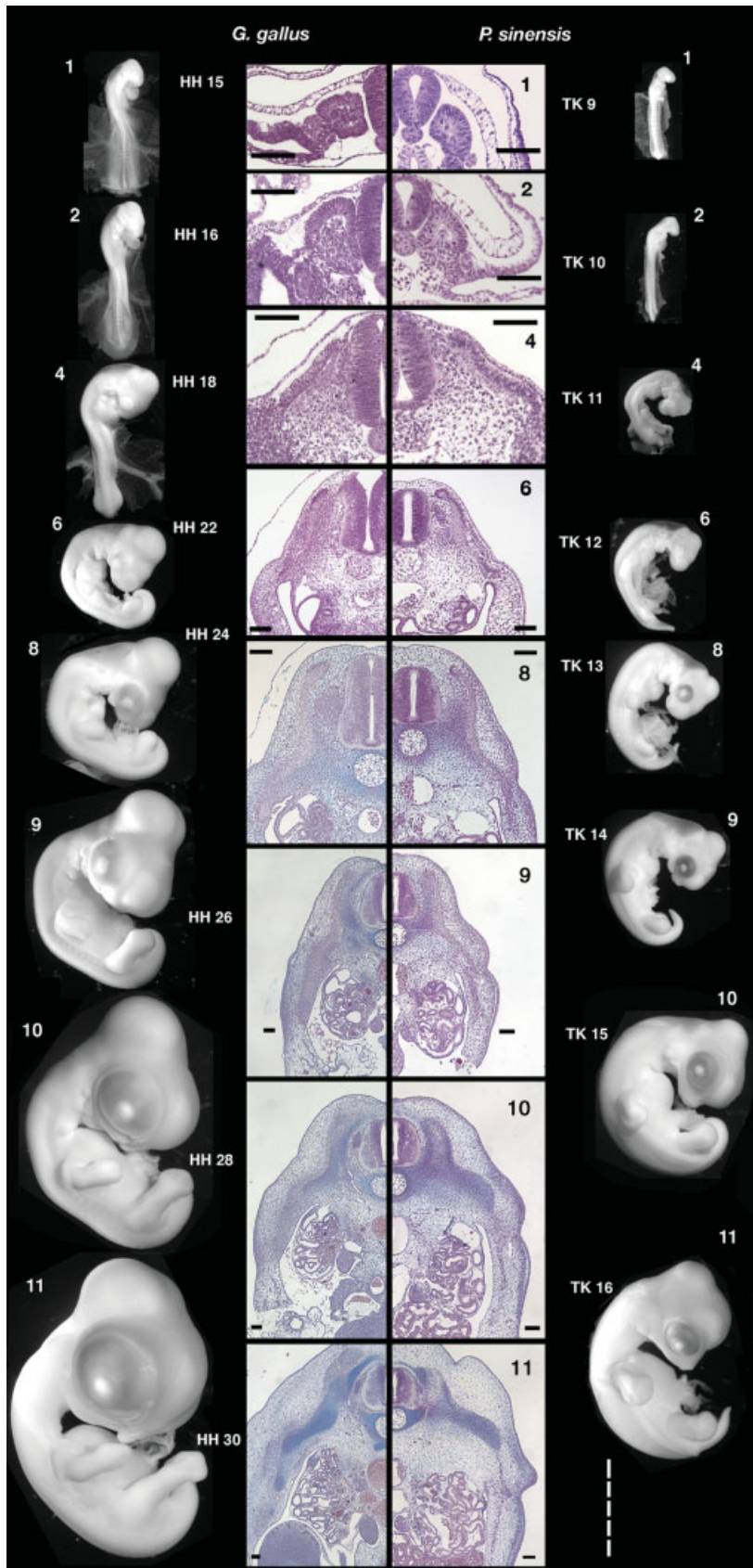
An anti-*P. sinensis* serum was raised as a cell-lineage marker with which to trace *P. sinensis* cells in the chimera. The serum obtained from chickens injected with homogenized *P. sinensis* embryos was applied to sectioned embryos of chicken and *P. sinensis* to determine its immunoreactivity. The antiserum clearly labeled all *P. sinensis* tissues but did not stain chicken tissues at all (Fig. 5). The staining pattern on *P. sinensis* was ubiquitous, although less dense on cartilage because

the cartilage matrices were not stained (data not shown). Labeling was predominant on cell surfaces and most of the epitopes were probably cell-membrane molecules. This finding is consistent with the fact that the labeling was lost or greatly reduced when high concentrations of detergent (Triton X-100) were used in the buffer (data not shown). Therefore, the antiserum could be used as a marker for embryonic *P. sinensis* cells.

Somitic Chimeras

In the chimeric embryos, the host thoracic somites were replaced with *P. sinensis* somites (Figs. 1, 6A). In the total of 93 chimeric embryos, 13 (14%) survived up to the stages when histological observations were performed. Six hours after surgery, the developmental rates of the host and donor somites appeared to be synchronized.

Two days after surgery, the donor somites had differentiated into sclerotomes and dermomyotomes with correct topographical orientation in the chimeric embryo, in all chimeras examined (Fig. 6B). Unlike the host somite on the control side, however, the donor sclerotome was associated with numerous blood vessels (Fig.



6B,C). These vessels were composed of *P. sinensis* endothelial cells, although blood cells were mostly of chicken origin (Fig. 6C). Mitotic cells were observed in both the sclerotomes and dermomyotomes on the chimeric side, although fewer in number than those on the control side (Fig. 6D–F). The differentiation of the donor somite described above appeared to be induced by the host embryonic environment, because the slightly older *P. sinensis* somites often self-differentiated into sclerotomes and dermomyotomes that were misoriented in the host (data not shown).

Five days after surgery, the chimera had developed to approximately PG stage 10 (Fig. 7G–I). By this stage, the graft-derived dermis had grown less extensively than that of the host, but was distributed in a pattern similar to the epaxial dermis observed in the chicken-quail chimera (Fig. 2D). The lateral limit of the graft-derived dermis did not correspond to the host ectodermal notch (Fig. 7H); this lack of correspondence was due to torsion in the chimeric embryo during postsurgical healing and does not necessarily represent a discrepancy with the notch that develops in the normal chicken embryos (Fig. 2A). This *P. sinensis* dermis was also limited epaxially and formed a rather clear boundary against the more ventral hypaxial dermis of host origin (Fig. 7H). As in the chicken, *P. sinensis* somite derivatives invaded the hypaxial region, where the *P. sinensis* cells differentiated into blood-vessel endothelial cells as well as into hypaxial muscle fibers (Fig. 7H,I). Except for the epaxial dermis, *P. sinensis* cells also formed part of the dorsal aorta, mesonephros, epaxial muscle, and the dense mesen-

Fig. 3. Comparison of embryonic development in *Pelodiscus sinensis* and *Gallus gallus*. Fixed embryos of *G. gallus* (left) and *P. sinensis* (right) are shown on either side of the figure, and histological images of comparable stages are shown in the middle. Compare with Table 1. Numbers indicate the common (*Pelodiscus* and *Gallus*) stages, and species-specific stages are prefixed by HH (Hamburger and Hamilton) for chicken and TK (Tokita and Kuratani) for *P. sinensis*. Not all the stages are shown here. Bars on the bottom right = 5 mm (each notch indicating 1 mm) for whole-mount embryos; and all the bars on histological sections = 100 μ m

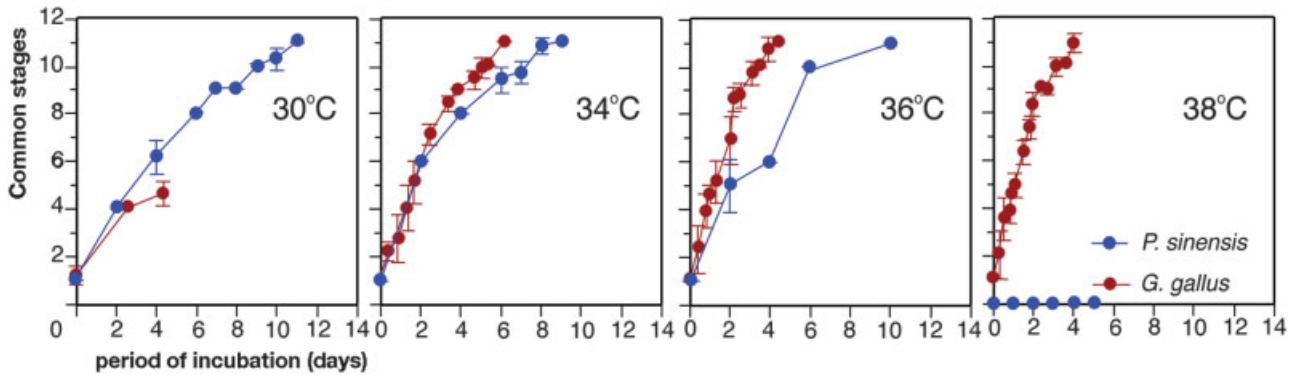


Fig. 4. Comparison of developmental rates. Developmental stages were plotted along a time scale between *Pelodiscus* and *Gallus* stages 1 to 11 for *Gallus gallus* and *Pelodiscus sinensis* raised at various temperatures. Dots and lines indicate developmental stages with standard deviations for *P. sinensis* (blue) and *G. gallus* (red). *Gallus gallus* stopped developing at temperatures below 30°C, and *P. sinensis* did not develop at temperatures above 38°C. Both species develop between 34°C and 36°C.

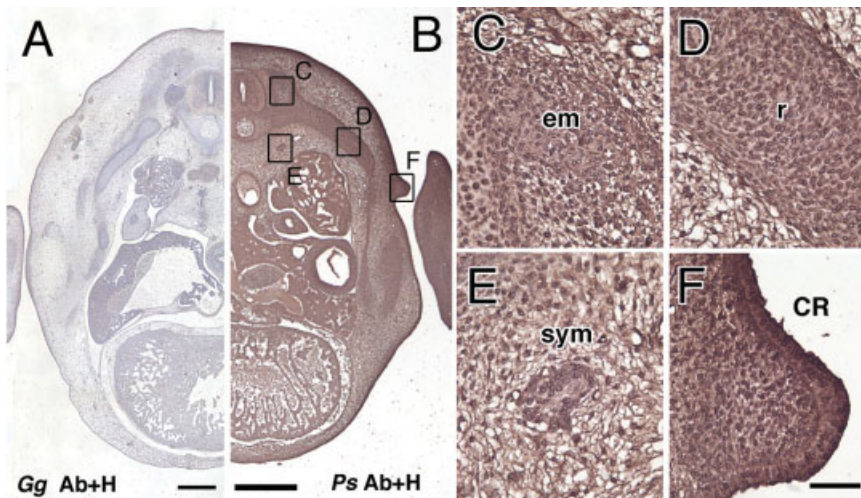


Fig. 5.

chyme at a site apparently corresponding to the site of neural-arch differentiation (Fig. 7H,I). *Pelodiscus sinensis* cells were never found in the dorsal root ganglia, which are neural-crest derivatives (data not shown; see below). We did not determine whether

Fig. 5. Species-specific immunoreactivity of anti-*Pelodiscus sinensis* IgY. **A,B:** Transverse sections of *Gallus gallus* (A) and *P. sinensis* (B) at the thoracic level stained with anti-*P. sinensis* antiserum (Ab), counterstained with hematoxylin (H). Note the species-specific immunoreactivity of the antiserum. **C-F:** High magnification of boxes in B, showing histology of the epaxial muscle (C), rib cartilage (D), sympathetic ganglion (E), and carapacial ridge (F) in *P. sinensis*. Scale bars = 500 μ m in A,B, 50 μ m in F (applies to C-F).

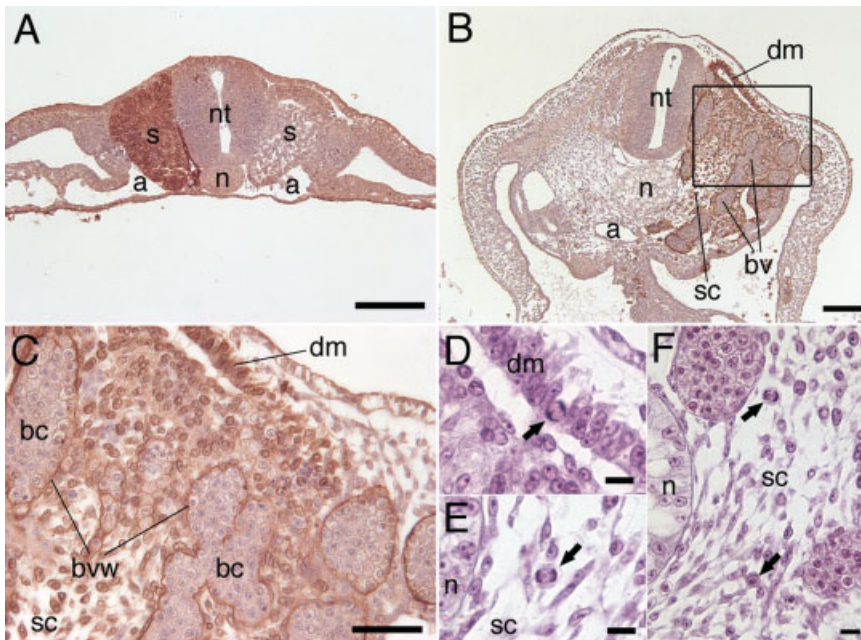


Fig. 6.

Fig. 6. Transplanted *Pelodiscus sinensis* somites. **A:** After 6 hr incubation after somite grafting between *P. sinensis* and *Gallus gallus*. A transverse section stained immunohistochemically with anti-*P. sinensis* antiserum and counterstained with hematoxylin. Note that the somite of the host is unilaterally replaced with a *P. sinensis* somite (s on the left). **B-F:** Two days after implantation of the *P. sinensis* somite in the chicken, shown on the right side. B and C are stained with anti-*P. sinensis* antiserum. The grafted somite has differentiated into a dermomyotome (dm) and sclerotome (sc), and numerous blood vessels (bv) have appeared on the operated side. C. High magnification of the box in B. Note that the endothelium of the blood vessels (bvw) is composed of *P. sinensis* cells, whereas the blood cells (bc) are chicken cells. D-F: Hematoxylin and eosin-stained sections from the specimen shown in B and C. D. An image of a mitotic epithelial cell in the *P. sinensis* somite-derived dermomyotome (arrow). E,F: Mitotic mesenchymal cells in the *P. sinensis* somite-derived sclerotome (arrows). a, dorsal aorta; n, notochord; nt, neural tube. Scale bars = 100 μ m in A,B, 50 μ m in C, 10 μ m in D-F.

P. sinensis cells formed any other skeletal tissues, although *P. sinensis* mesenchyme tended to be aggregated around the host notochord and at the site of prospective neural-arch development (Fig. 7H,I).

Seven days after surgery, the *P. sinensis* somites contributed to the same repertoire of embryonic tissues as observed in the 5-day chimeras (Fig. 7J,M,N). Dorsal root ganglia were never populated by *P. sinensis* cells (Fig. 7M). The MF-20-positive epaxial and hypaxial muscles were also derived from *P. sinensis* somites (Fig. 7B,C,E,F), and by this stage, the latter muscle had differentiated into a thin sheet of muscle fibers (Fig. 7M,N). The overall morphology of this muscle more closely resembled the *P. sinensis* hypaxial muscle shown in Figure 2B than that of the host (Fig. 2A). A few cartilage nodules were composed of *P. sinensis* cells, associated with host cartilage, but no larger *P. sinensis* cartilage was found with the normal morphology of ribs or vertebrae (Fig. 7M,N). Those small pieces of *P. sinensis* cartilage had no extensive extracellular matrix that could be stained with Alcian blue, as did the host cartilage (Fig. 7K,L). No ribs were derived from *P. sinensis* somites at this stage. In chimeras that had received somites and the overlying surface ectoderm of *P. sinensis*, ribs derived from the graft were not observed at even 7 days after the surgery (3 embryos survived of 21 chimeras constructed; data not shown).

Expression of *Shh* and *Pax9* Orthologues

To determine whether the differences in cartilage differentiation between *P. sinensis* and host somites in the chimera were due to differences in inductive signaling derived from the notochord, the expression of *Shh* was examined (Fig. 8A–D). At PG stages 4 to 8, *Shh* orthologues were specifically and strongly up-regulated in both species in the floor plate of the neural tube and in the notochord, suggesting that the gene is involved in the patterning of the mesoderm at similar stages of embryonic development in both species, with shared embryonic topography.

To examine whether the implanted

P. sinensis somites responded to the signals derived from *Shh*, expression of *Pax9* was observed in chimeras that had been incubated for 3 days after surgery (Fig. 8E). An antisense probe for *P. sinensis Pax9* detected high levels of transcripts in the sclerotomes of both chicken and *P. sinensis* (the probe also recognized chicken *Pax9* transcripts).

DISCUSSION

Despite its evolutionary importance, experimental embryological studies of the turtle are rare (Yntema, 1970; Fallon and Crosby, 1977; Burke, 1991), partly due to the difficulties in the collection and handling of turtle eggs and to a lack of cell-lineage markers. In the present study, we raised anti-*P. sinensis* polyclonal IgY for the first time. It specifically recognized tissues of *P. sinensis*, allowing us to determine the developmental fates of *P. sinensis* grafts in chimeras at the cellular level (Figs. 5–7). Another problem associated specifically with interspecific chimeras is the incompatibility of developmental time tables; the development of different animals proceeds at different rates at different temperatures. A well-known example is the chimera between *Xenopus* and axolotl, which cannot be grown to advanced stages (Armstrong and Muneoka, 1989). The same problem was encountered in the present study. In chicken–turtle chimera, Fallon and Crosby (1977) reported that the zone of polarizing activity (ZPA) from the limb buds of *Cherydra serpentina* and *Chrysemys picta* was able to function in the chicken host. In these experiments, however, the tissue differentiation of the graft was not observed, and only the ZPA-derived signaling molecules appeared to have acted on the chicken limb buds. Actually, when incubated at 38°C, the *P. sinensis* somite could form only a small mesenchymal cell population in the chicken host environment even 5 days after the surgery (data not shown). To overcome species-specific differences in the developmental time tables, we first identified the common developmental stages based on the developmental patterning of somite derivatives at the histological level and identified 34–36°C as the appropriate

range of temperatures at which both species could grow to histogenetic stages (Fig. 4). The incompatibility of tissue interactions will be discussed below, especially in the context of cartilage development in the chimera.

Chimeric surgery was apparently successful in the present study. In both the *G. gallus*–*C. coturnix* and *G. gallus*–*P. sinensis* chimeras, graft-derived cells occupied the space lateral to the notochord, showing that the host tissue to be replaced had been removed properly (Figs. 2, 6A,B, 7H,K,M). Furthermore, tissues known to be derived from somites were replaced with grafted cells (Figs. 6, 7): in the chimeras constructed between avian embryos, grafted somites contribute to the endothelium of blood vessels, including the dorsal aorta and those in the mesonephros (Wilting et al., 1995; Pardanaud et al., 1996; Ambler et al., 2001). In quail–mouse chimeras, however, mouse somite (graft)-derived cells never contributed to the endothelium (Ambler et al., 2001). The occasional presence of donor cells in the dorsal aorta and mesonephros in the present study is reminiscent of inter-avian species chimera cited above, showing a possibility that *P. sinensis* somites could respond to avian vascular patterning signals. Extensive development of blood vessels on the experimental side of the chimera could be due to the wound-healing after the surgery: during the removal of host somites, the host embryo often bled.

Appearance of *P. sinensis* cells in the mesonephric ducts of the chimera (Fig. 7H,I), on the other hand, may not reflect the normal differentiation of the somites in either animal, but this might be explained by the induction of intermediate mesoderm in the grafted tissue by the host environment. The host intermediate mesoderm was damaged during surgery, altering the developmental fates of the grafted somites. Lateral mesoderm is capable of inducing *Pax-2* expression, a marker for intermediate mesoderm, in the somites when these mesodermal tissues are cocultures (James and Schultheiss, 2003).

One of the most conspicuous elements in the turtle embryo of turtle-specific morphology is the presence of the CR in the embryonic trunk (Figs.

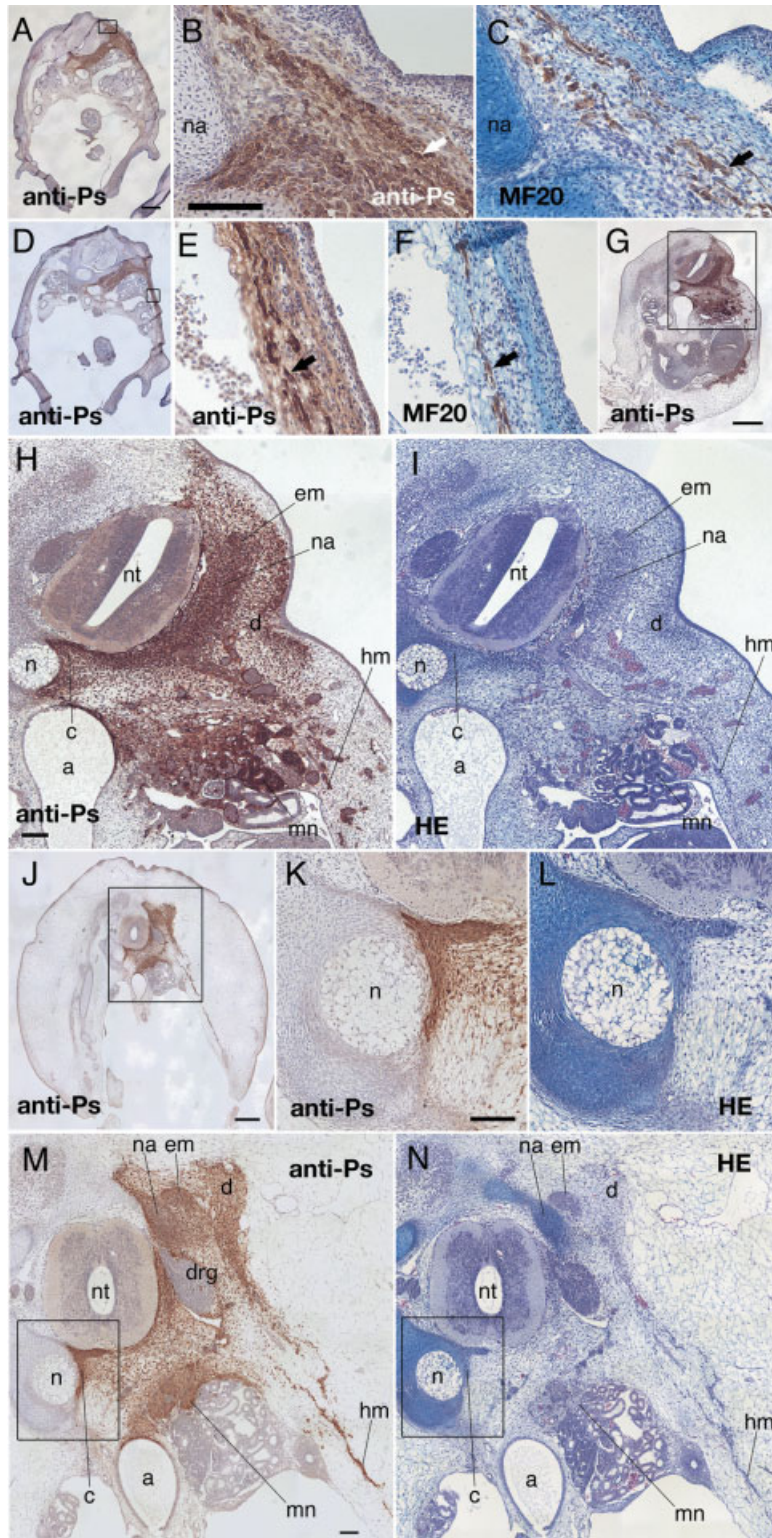


Fig. 7.

2, 3); no such structure is apparent in the chicken embryo. By comparative morphology and construction of chicken-quail chimeras, we determined that the CR probably develops

at the junction of the epaxial and hypaxial regions (or at the dorsal limit of the lateral body wall; Fig. 2). The mesenchyme of the CR itself appears to be composed of somite-derived cells,

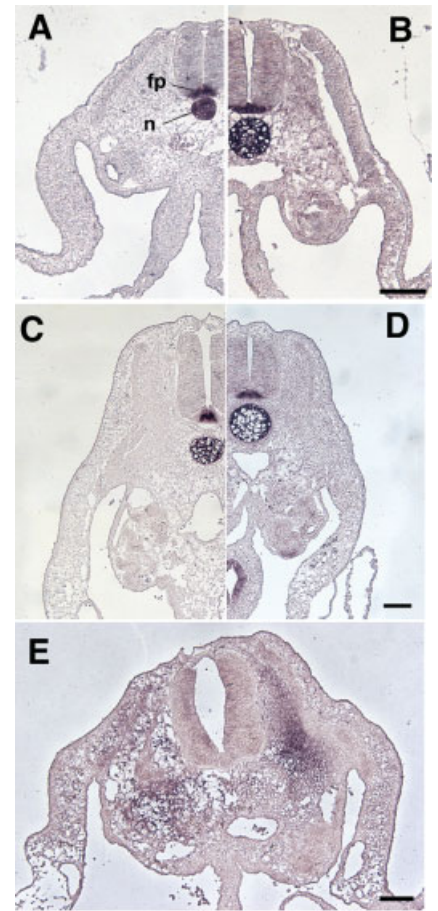


Fig. 8. Comparison of *Shh* and *Pax9* gene expression patterns. **A–E:** Expression patterns of *Shh* homologues were compared at the thoracic levels of *Pelodiscus* and *Gallus* stage 4 (**A,B**) and stage 8 (**C,D**) embryos of *Gallus gallus* (**A,C**) and *Pelodiscus sinensis* (**B,D**), and *Pax9* expression was examined in the chimera in which the left somite had been replaced with a somite of *P. sinensis* (**E**). An antisense riboprobe for *P. sinensis Pax9* also recognized chicken *Pax9* transcripts in the chicken host. **A–D:** The *Shh* genes are highly up-regulated in the floor plate (fp) of the neural tube and in the notochord (n) in both species. **E:** In the chimera, somites have differentiated into dermomyotomes and sclerotomes on both sides, and *Pax9* is up-regulated specifically in the sclerotomes. The disorganized histology of the *P. sinensis* sclerotome reflects the hypertrophic development of blood vessels derived from the graft (also see Fig. 6B,C). Histological observations were made on transversely sectioned specimens at the levels of somites (s) 15–21 for *P. sinensis* and s22–26 for *G. gallus* (see Fig. 3). TK stages refer to the developmental stages of *P. sinensis* described by Tokita and Kuratani (2001), and HH stages to those described by Hamburger and Hamilton (1951) for *G. gallus* development. The common stages were established on the basis of the developmental patterning of somites. Scale bars = 100 μ m in B (applies to A,B), in D (applies to C,D), in E.

namely the epaxial dermis (Fig. 3). In the present study, *P. sinensis* somites differentiated into the epaxial dermis, although not as extensively as in the host dermis (Fig. 7H). However, whether the *P. sinensis* dermis could self-differentiate or induce the CR in the chicken host remains unanswered in the present study, mainly because the morphology of the chimeras was distorted (Fig. 7G–I). This finding is partly caused by the differential developmental rates of the dermis, an inherent problem specifically associated with the construction of interspecific chimeras. To address this question, CR-specific marker genes (Loredo et al., 2001; Vincent et al., 2003) should be isolated and their expression (or the expression of their chicken homologues) should be analyzed in the chimeras, which we are undertaking in a future project.

The present chimeric study was expected to identify the turtle-specific developmental program that proceeds within the somite-derived cells themselves—the cell-autonomous programs in somite derivatives, such as the muscles and ribs. These structures show species-specific differences in morphology in chicken and turtle (Fig. 2). The key question is whether this specific morphology is inherent to the somite-derived cells (predetermined in the somites) or if it requires species-specific interactions with the embryonic environment. The development and differentiation of *P. sinensis*

somites, when exposed to the chicken environment, might identify the part of the turtle-specific developmental program that is predetermined within the somites, as will be discussed below.

The amniote somite undergoes hierarchical steps in its differentiation in response to signals derived from the embryonic environment. For the initial differentiation of the epithelial somite into the sclerotome and dermomyotome, the signal from the notochord that induces deepithelialization of the ventromedial part of the somite to form the sclerotome is indispensable (Brand-Saberi et al., 1993; Goulding et al., 1994; Ebensperger et al., 1995; also see: Fan and Tessier-Lavigne, 1994; Christ and Ordahl, 1995). In the present study, the *P. sinensis* somite, which at the stage of transplantation is epithelial, was capable of responding to such a signal, because it always differentiated into the sclerotome and dermomyotome with the appropriate polarity; with dermomyotome beneath the ectoderm, and sclerotome near the notochord (Fig. 6B). Slightly older *P. sinensis* somites often self-differentiated into those subdivisions with an inappropriate polarity (the dermomyotome lateral to the neural tube, for example). This finding suggests that early *P. sinensis* somites (somite stages +I to +III) are perfectly competent to respond to the signals derived from the chicken embryonic environment, con-

sistent with the ability of young somites (before stage II) to reorientate, as reported for chicken embryos (Aoyama and Asamoto, 1988).

Further differentiation of the somite involves the formation of several cell types, such as the dermis, chondrocytes, and myofibrils, which again requires signals derived from the embryonic environment (Koseki et al., 1993; Goulding et al., 1994; Ebensperger et al., 1995). We determined histologically that the *P. sinensis* somites in the chimera gave rise to all these expected cell types (Figs. 6, 7). Moreover, in muscle differentiation, the histogenesis of *P. sinensis* somite derivatives appeared to follow, not the pattern of the chicken, but that of *P. sinensis*. This differentiation was especially apparent in the hypaxial part (Figs. 2A,B, 7M,N). Therefore, it seems very reasonable to assume that the turtle-specific patterning of the trunk muscles is more or less governed by a cell-autonomous developmental process, although it requires preceding inductive events controlled by the host environment. Similar cell-autonomous differentiation of myofibrils has also been reported in chicken–quail chimeric experiments (Nikovits et al., 2001). Alternatively, the poor development of the hypaxial muscles in the chimera could have been due to the inability of the turtle myoblasts to respond to the host embryonic environment, which in turn could be one of the changes introduced to the developmental program of the muscles in the turtle ancestors. Species-specific morphogenesis of muscles may be more reminiscent of crest cell-autonomous craniofacial patterning as demonstrated by Schneider and Helms (2003), who exchanged the cephalic neural crest between quail and duck and obtained graft-specific craniofacial morphology in the chimeric animals.

In contrast, the skeletogenesis of the *P. sinensis* somite was strongly arrested in the chimera described here (Fig. 7). It is hardly conceivable that the chimeras were not incubated long enough for *P. sinensis* cells to proceed chondrification: when TK stage 9 embryos were incubated at 34 to 36°C for 7 days, they reach PG stage 10, when cartilage primordia can be readily seen as overt condensations of

Fig. 7. Histogenesis of *P. sinensis* somite in the chimera. Transverse sections of a *Pelodiscus sinensis*–*Gallus gallus* chimera. Sections are cut at the site of graft and either stained with anti-*P. sinensis* antiserum and counterstained with hematoxylin (A,B,D,E,G,H,J,K,M), immunostained with MF-20 antibody and counterstained with hematoxylin and Alcian blue (C,F), or simply stained with hematoxylin and eosin and then Alcian blue (I,L,N). **A–F:** *P. sinensis* somite-derived muscles in 7-day chimera. B and C are adjacent sections at higher magnification corresponding to the box in A, showing *P. sinensis* somite-derived epaxial muscle (arrows in B and C). At this level, the neural arch (na) and ribs are of host tissue. E and F are adjacent sections at higher magnification corresponding to the box in D, similarly showing the hypaxial muscle (arrows in E and F). Only the muscle fibers are of *P. sinensis* somite origin. **G:** Transverse section of a chimera incubated for 5 days. **H,I:** Adjacent sections corresponding to the box in G at high magnification. *Pelodiscus sinensis* somite-derived cells are observed in the dermis (d), dorsal wall of the dorsal aorta (a), mesenchyme, corresponding to the site of neural arch development (na), epaxial muscle primordium (em), prospective centrum (c), putative hypaxial muscle (hm), and mesonephros (mn). **J–N:** Seven days after surgery. K is a higher magnification of the box in M, which is a higher magnification of the box in J. L and N are sections adjacent to K and M, respectively. *P. sinensis* cells occur in tissues known to be somite derivatives (M and N). Neural crest-derived dorsal root ganglion (drg) is composed of chicken cells (M). Note that only a small population of *P. sinensis* cells on the right side of the host notochord (n; K) has differentiated into a small cartilage, stained with Alcian blue (L). Also note that the *P. sinensis* somite-derived hypaxial muscle (hm) more strongly resembles the muscle in the normal *P. sinensis* embryo than that in the chicken embryo (compare Fig. 2A and 2B). nt, neural tube. Scale bars = 500 μ m in A (applies to A,D), in G, in J, 100 μ m in B (applies to B–F), in H (applies to H,I), in K (applies to K,L), in M (applies to M,N).

mesenchyme (see Figs. 4, 7M,N). Furthermore, as seen in chimeras incubated for 5 days, development of *P. sinensis* somite-derivatives and host tissues synchronized well when compared with the chick-quail chimeras grown for the same period (Figs. 2C, D, 7G–I). It is likely, thus, that the length of incubation of the turtle-chick chimeras is sufficient to allow turtle cells to chondrify. Cartilage condensations are readily visible in turtle embryos that have been similarly incubated.

It has long been known that chondrogenesis is dependent also upon the embryonic environment (Hoadley, 1925; Williams, 1942; Fowler and Watterson, 1953; Watterson et al., 1954; Avery et al., 1955, 1956; Kenny-Mobbs and Thorogood, 1987) and apparently proceeds in hierarchical interactive steps. For example, chondrification of the centrum involves active migration of the early sclerotome-derived cells toward the notochord (Williams, 1910; Jacob et al., 1975; Chernoff and Lash, 1981), where the extracellular matrix (ECM) plays an important role (Newgreen et al., 1986; Lash et al., 1987; Sanders et al., 1988). In the chimeras of the present study, this process also seems to have taken place, because *P. sinensis* cells often aggregated normally, lateral to the notochord (Figs. 6A,B, 7H,M). An aggregation of *P. sinensis* cells corresponding to the shape of the prospective neural arch was also observed (Fig. 7H,I). However, these cells did not show normal chondrification. A series of experiments in chicken embryos showed that there are certain developmental stages at which sclerotome-derived cells are able to chondrify without signals from the embryonic environment (Fowler and Watterson, 1953; Watterson et al., 1954; Avery et al., 1956; O'Hare, 1972; Kenny-Mobbs and Thorogood, 1987). Therefore, it appears that *P. sinensis* cells failed to reach those particular stages in the present chimera. The environmental factors required to bring *P. sinensis* cells to these stages remain unknown.

As described above, the reduction in *P. sinensis* somite-derived cartilage did not arise from an incapacity for chondrocyte differentiation of the *P. sinensis* somitic cells per se in the host

environment, because *P. sinensis* chondrocytes were observed (Fig. 7K–M). These minor cartilaginous nodules were always associated with host cartilage (Fig. 7K,M), suggesting that they were induced through local, cell-cell contact-dependent homogenetic induction, which has been reported previously in chondrogenesis (Cooper, 1965). Although we transplanted the *P. sinensis* somites together with the covering surface ectoderm that has been assumed to function in inducing rib differentiation (Huang et al., 2000 and references therein), no ribs were found in these chimeras, either.

The general absence of graft-derived cartilage in the chimera is probably due to an incompatibility between the chicken environment and the chondrogenic mesenchyme derived from the *P. sinensis* somites. We do not know if this incompatibility is due to the signaling system or to differences between these species in the molecules themselves that are involved in the same signaling mechanism or act as components of the ECMs. Nor is it known whether such differences are relevant to the turtle-specific pattern of rib growth. There was no clear difference in the expression patterns of *Shh* beyond the stage of sclerotome formation (Fig. 8A–D), although the gene products may function differently in the two species. Furthermore, up-regulation of *Pax9* in the graft-derived sclerotome shows that the mesodermal cells of *P. sinensis* could normally respond to some of the signals derived from *G. gallus*, including the product of the *Shh* gene (Fig. 8E). In this context, it would be worthwhile to consider the anatomical difference of ribs between turtles and other amniotes. Namely, as found by Goette (1899), the development of the ribs and neural arches of turtles has shifted rostrally by a half segment when compared with other amniotes, and segmental patterns of muscular, nervous, and skeletal systems have been accordingly reorganized secondarily in the turtle lineage (Hoffstetter and Rage, 1969). Such a difference might have disturbed the normal patterning of the ribs in the chimera. Even in that circumstance, however, the middle segment of the transplanted three somites could have generated a normal turtle rib. However,

this does not explain the occasional appearance of *P. sinensis*-derived neural arch in the chimera or the specific loss of ribs. Lastly, the poor development of cartilage in the chimera might be related to the widely recognized fact that maintenance of cartilage differentiation in a culture system tends to require finely tuned extracellular conditions (Daniels and Solursh, 1991, and references therein), in marked contrast to muscle differentiation. An investigation of the differences between the embryonic factors of *P. sinensis* and *G. gallus* will be included in our future project.

EXPERIMENTAL PROCEDURES

Embryos

Fertilized eggs of *P. sinensis* were obtained from several local fish farms in Japan during the breeding seasons (June to September) of 2002 and 2003. The eggs were allowed to grow in a humidified incubator (for temperatures, see below). Developmental stages (TK stages) were determined based on the previous description by Tokita and Kuratani (2001). Fertilized eggs of the chicken *G. gallus* and the Japanese quail *Coturnix coturnix* were also purchased from a local farm, and the eggs were incubated in a humid temperature-controlled chamber. The embryos were staged according to Hamburger and Hamilton (1951). To establish the common stages between chicken and *P. sinensis*, hematoxylin and eosin (H&E)-stained sections were analyzed histologically (see below). Based on this developmental time table, the eggs of both species were incubated at different temperatures to determine the appropriate conditions under which chimeras should be incubated (see below).

Construction of Chimeras

Chick embryos incubated for 2.5 days at 38°C (24–26 somites, HH stage 15; Hamburger and Hamilton, 1951) were used as the host. A window was made in the shell and the embryo was visualized with Indian ink diluted with 0.9% NaCl/distilled water (1:5) injected into the subgerminal cavity. With a sharpened tungsten needle,

the surface ectoderm over the three newly developed somites was peeled unilaterally (somite stages +I to +III at the thoracic level; Roman numerals indicate the positions of somites counted rostrally from the most newly formed one that is called somite +I; Ordahl, 1993), and a few drops of Dispase (500 IU/mL in Tyrode's solution; Godo Shusei Co., Ltd., Tokyo, Japan) were applied to the scar. After 5 min, the three somites were removed using a tungsten needle and a glass capillary pipette. From the thoracic level of a *P. sinensis* embryo that had been incubated for 2 days at 30°C (17–21 somites, TK stage 9), three somites at stages +I to +III were excised from the corresponding side with Dispase, rinsed in 0.9% NaCl/distilled water, and placed into the scar of the chicken host along the same anteroposterior axis (Fig. 1). Surgery was always performed unilaterally, and the nonoperated side was used as the control. Thirteen successful chimeras were used for analysis. Similar transplantation of somites was also carried out between chicken and quail embryos (quail somites into chicken hosts) for comparison.

Anti-*P. sinensis* Antiserum

P. sinensis embryos were collected at TK stage 14, homogenized, and injected into an adult female chicken. Serum was collected approximately 3 months later (Sawady Technology, Tokyo, Japan). For immunohistochemistry, embryos were fixed in either 4% paraformaldehyde (PFA) in phosphate-buffered saline (PBS; pH 7.4) or Bouin's fixative, then dehydrated, and embedded in paraffin. Deparaffinized sections (6 µm) were incubated with the anti-*P. sinensis* antiserum (1:300) for 2 hr at room temperature. Horseradish peroxidase (HRP)-conjugated anti-chicken IgY (Bethyl Laboratories, Montgomery, TX) was used as the secondary antibody. HRP reactivity was visualized with the diaminobenzidine reaction.

Immunohistochemistry and Histochemistry

Histological observations were made mainly on H&E-stained sections, which were often further stained with

0.1% Alcian blue/distilled water, according to the method of Nowicki et al. (2003), to show the cartilage in older embryos. To detect quail cells in chicken-quail chimeras, the quail-specific antibody, QCPN (1:5; Developmental Studies Hybridoma Bank [DSHB]) was used on embryos fixed with Serra's fixative (Serra, 1946). For immunohistochemistry with MF-20 antibody (DSHB), which recognizes tropomyosin, embryos were fixed with 4% PFA/PBS, and 10-µm-thick sections were prepared with a cryostat. Staining was performed by using the method described by Kuratani and Wall (1992). Biotin-conjugated anti-mouse IgG1 (Zymed, South San Francisco, CA) was used as the secondary antibody. Vectastain ABC Elite kit (Vector Laboratories, Burlingame, CA) was used to visualize the immunoreaction. All histological images were taken using a CoolSNAP camera (RS Photometrics, Tucson, AZ) attached to a light microscope.

Isolation and Sequencing of *Shh* and *Pax9* cDNAs and In Situ Hybridization

Total RNAs isolated from TK stage 14 *P. sinensis* embryos were reverse-transcribed into cDNAs by using oligo(dT) primer with SuperScript III (Invitrogen, Carlsbad, CA). These cDNAs were used as templates for polymerase chain reaction (PCR) amplification with the Expand High Fidelity PCR System (Roche, Penzberg, Germany). Degenerate primers were designed based on conserved amino acid residues as follows (corresponding amino acids in parentheses): 5'-CTGACGCCNYTNGCNTAYAARCARTT-3' (PLAYKQF) and 5'-TTCGCGCTCANSWRITTYTCNGCYTT-3' (KAENVA) for *Shh*; and 5'-GATCCNGGNATHHTTYGCNTGGGAR AT-3' (GIFAWEI) and 5'-GTATACGGCATRTANGGNSWNACYTG-3' (QVSPYM) for *Pax9*. PCR was performed as follows: 2 min denaturation step at 94°C; then 10 cycles of 94°C for 15 sec, 48°C for 30 sec, and 72°C for 2 min; followed by 30 cycles of 94°C for 15 sec, 56°C for 30 sec, and 72°C for 2 min. The PCR products were purified by using MinElute (Qiagen, Hilden, Germany) and cloned into the pT7Blue vector (Novagen, Madison, WI). More than three independent clones were isolated

and sequenced with the 3100 Genetic Analyzer (Applied Biosystems, Foster City, CA). The orthology of *P. sinensis Shh* and *Pax9* cognates, including the amino acid sequences deduced from the cDNAs isolated and sequenced as described above, were confirmed by comparison with those reported for other vertebrates using analysis of phylogenetic trees (these sequences were deposited in GenBank with accession nos. AB181135 and AB181136).

For in situ hybridization, embryos were embedded in paraffin after fixation, sections (6 µm) were cut, and the deparaffinized sections were treated with 0.1 M triethanolamine/1.0% HCl/0.2% acetic anhydride. After incubation in hybridization buffer (50% formamide, 5 × standard saline citrate (SSC), 1% sodium dodecyl sulfate, 0.05 mg/ml total yeast RNA, 50 mg/ml heparin sulfate, 5 mM ethylenediaminetetraacetic acid-Na₂, 0.1% CHAPS; Murakami et al., 2001) for 2 hr at 65°C, slides were incubated in hybridization buffer containing digoxigenin-labeled RNA probe (0.1 µg/µl) at 65°C overnight. Sections were washed in 0.2× SSC at 65°C and at room temperature for 30 min each, incubated in 1% Blocking Reagent (Roche) for 60 min, and then incubated with Anti-Digoxigenin-AP Fab Fragment (Roche) diluted in 1% Blocking Reagent (1:4,000) at room temperature for 2 hr. The antibody detection reaction was performed as previously described (Murakami et al., 2001).

ACKNOWLEDGMENTS

We thank Raj Ladher, Kiyokazu Agata, and Yoshie Kawashima Ohya for critical reading of the manuscript, and Takeshi Inoue for technical advice. The monoclonal antibodies (MF20 developed by Donald A. Fischman; QCPN by Bruce M. Carlson and Jean A. Carlson) were obtained from the Developmental Studies Hybridoma Bank developed under the auspices of the NICHD and maintained by the Department of Biological Sciences, University of Iowa, Iowa City, IA 52242. S.K. was funded by Grants-in-Aid from the Ministry of Education, Science and Culture of Japan (Specially Promoted Research).

REFERENCES

- Ambler CA, Nowicki JL, Burke AC, Bautch VL. 2001. Assembly of trunk and limb blood vessels involves extensive migration and vasculogenesis of somite-derived angioblasts. *Dev Biol* 234:352–364.
- Aoyama H, Asamoto K. 1988. Determination of somite cells: independence of cell differentiation and morphogenesis. *Development* 104:15–28.
- Armstrong JB, Muneoka K. 1989. Genetic markers and their use in chimeras. In: Armstrong JB, Malacinski GM, editors. *Developmental biology of the axolotl*. New York: Oxford University Press. p 236–254.
- Avery G, Chow M, Holtzer H. 1955. Comparison of the salamander and chick notochords in the differentiation of somitic tissues. *Anat Rec* 122:444.
- Avery G, Chow M, Holtzer H. 1956. An experimental analysis of the development of the spinal column. V. Reactivity of chick somites. *J Exp Zool* 132:409–426.
- Brand-Saberi B, Ebensperger C, Wilting J, Balling R, Christ B. 1993. The ventralizing effect of the notochord on somite differentiation in chick embryos. *Anat Embryol (Berl)* 188:239–245.
- Brent AE, Tabin CJ. 2002. Developmental regulation of somite derivatives: muscle, cartilage and tendon. *Curr Opin Genet Dev* 12:548–557.
- Burke AC. 1989. Development of the turtle carapace: implications for the evolution of a novel bauplan. *J Morphol* 199:363–378.
- Burke AC. 1991. The development and evolution of the turtle body plan: inferring intrinsic aspects of the evolutionary process from experimental embryology. *Am Zool* 31:616–627.
- Burke AC, Nowicki JL. 2003. A new view of patterning domains in the vertebrate mesoderm. *Dev Cell* 4:159–165.
- Cao Y, Sorenson MD, Kumazawa Y, Mindell DP, Hasegawa M. 2000. Phylogenetic position of turtles among amniotes: evidence from mitochondrial and nuclear genes. *Gene* 259:139–148.
- Chernoff EAG, Lash JW. 1981. Cell movement in somite formation and development in the chick: inhibition of segmentation. *Dev Biol* 87:212–219.
- Christ B, Ordahl CP. 1995. Early stages of chick somite development. *Anat Embryol (Berl)* 191:381–396.
- Christ B, Wilting J. 1992. From somites to vertebral column. *Ann Anat* 174:23–32.
- Christ B, Jacob HJ, Jacob M. 1974. Experimentelle Untersuchungen zur Entwicklung der Brustwand beim Hühnerembryo. *Experientia (Basel)* 30:1449–1451.
- Christ B, Huang R, Wilting J. 2000. The development of the avian vertebral column. *Anat Embryol (Berl)* 202:179–194.
- Cooper GW. 1965. Induction of somite chondrogenesis by cartilage and notochord; A correlation between inductive activity and specific stages of cytodifferentiation. *Dev Biol* 12:185–212.
- Daniels K, Solorsh M. 1991. Modulation of chondrogenesis by cytoskeleton and extracellular matrix. *J Cell Sci* 100:249–254.
- Dockter JL. 2000. Sclerotome induction and differentiation. *Curr Top Dev Biol* 48:77–127.
- Ebensperger C, Wilting J, Brand-Saberi B, Muzutani Y, Christ B, Balling R, Koseki H. 1995. *Pax-1*, a regulator of sclerotome development is induced by notochord and floor plate signals in avian embryos. *Anat Embryol (Berl)* 191:297–310.
- Emelianov SW. 1936. Die Morphologie der Tetrapodenrippen. *Zool Jahrb Abt Anat Ont Tiere* 62:173–274.
- Evans DJR. 2003. Contribution of somitic cells to the avian ribs. *Dev Biol* 256:114–126.
- Ewert MA. 1985. Embryology of turtles. In: Gans C, Billet F, Maderson PFA, editors. *Biology of the reptilia* 14. New York: John Wiley and Sons. p 74–255.
- Fallon JF, Crosby GM. 1977. Polarising zone activity in limb buds of amniotes. In: Ede DA, Hinchliffe JR, Balls M, editors. *Vertebrate limb and somite morphogenesis*. Cambridge: Cambridge University Press. p 55–69.
- Fan C-M, Tessier-Lavigne M. 1994. Patterning of mammalian somites by surface ectoderm and notochord: evidence for sclerotome induction by a hedgehog homolog. *Cell* 79:1175–1186.
- Fowler I, Watterson RL. 1953. The role of the neural tube in development of the axial skeleton of the chick. *Anat Rec* 117:555–556.
- Gilbert SF, Loreda GA, Brukman A, Burke AC. 2001. Morphogenesis of the turtle shell: the development of a novel structure in tetrapod evolution. *Evol Dev* 3:47–58.
- Goette A. 1899. Über die Entwicklung des knöchernen Ruckenschildes (Carapax) der Schildkroten. *Z wiss Zool* 66:407–434.
- Goulding MD, Lumsden A, Paquette AJ. 1994. Regulation of *Pax-3* expression in the dermomyotome and its role in muscle development. *Development* 120:957–971.
- Haeckel E. 1875. Die Gastrea und die Eifurchung der Thiere. *Jena Z Naturwiss* 9:402–508.
- Hall BK. 1998. *Evolutionary developmental biology*. 2nd ed. London: Chapman and Hall. 491 p.
- Hamburger V, Hamilton HL. 1951. A series of normal stages in the development of the chick embryo. *J Morphol* 88:49–92.
- Hedges SB, Poling LL. 1999. A molecular phylogeny of reptiles. *Science* 283:998–1001.
- Hoadley L. 1925. The differentiation of isolated chick primordia in chorio-allantoic grafts. II. The effect of the presence of the spinal cord, i.e., innervation, on the differentiation of the somitic region. *J Exp Zool* 42:143–162.
- Hoffstetter R, Rage J-C. 1969. Vertebrae and ribs of modern reptiles. In: Gans C, Bellaris Ad'A, Persons TS, editors. *Biology of the reptilia* 1. London: Academic Press. p 201–310.
- Huang R, Zhi Q, Wilting J, Christ B. 1994. The fate of somitocoel cells in avian embryos. *Anat Embryol (Berl)* 190:243–250.
- Huang R, Zhi Q, Neubuser A, Muller TS, Brand-Saberi B, Christ B, Wilting J. 1996. Function of somite and somitocoel cells in the formation of the vertebral motion segment in avian embryos. *Acta Anat* 155:231–241.
- Huang R, Zhi Q, Schmidt C, Wilting J, Brand-Saberi B, Christ B. 2000. Sclerotomal origin of the ribs. *Development* 127:527–532.
- Jacob M, Jacob H, Christ B. 1975. The early differentiation of the perinotochordal connective tissue. A scanning and transmission electron microscopic study on chick embryos. *Experientia* 31:1083–1086.
- James RG, Schultheiss TM. 2003. Patterning of the avian intermediate mesoderm by lateral plate and axial tissues. *Dev Biol* 253:109–124.
- Kato N, Aoyama H. 1998. Dermomyotomal origin of the ribs as revealed by extirpation and transplantation experiments in chick and quail embryos. *Development* 125:3437–3443.
- Kenny-Mobbs T, Thorogood P. 1987. Autonomy of differentiation in avian brachial somites and the influence of adjacent tissues. *Development* 100:449–462.
- Koseki H, Wallin J, Wilting J, Mizutani Y, Kispert A, Ebensperger C, Herrmann BG, Christ B, Balling R. 1993. A role for *Pax-1* as a mediator of notochordal signals during the dorsoventral specification of vertebrae. *Development* 119:649–660.
- Kumazawa Y, Nishida M. 1999. Complete mitochondrial DNA sequences of the green turtle and blue-tailed mole skink: statistical evidence for archosaurian affinity of turtles. *Mol Biol Evol* 16:784–792.
- Kuratani SC, Wall NA. 1992. Expression of Hox 2.1 protein in a restricted population of neural crest cells and pharyngeal ectoderm. *Dev Dyn* 194:15–28.
- Lash JW, Linask KK, Yamada KM. 1987. Synthetic peptides that mimic the adhesive recognition signal of fibronectin: differential effects on cell-cell and cell-substratum adhesion in embryonic chick cells. *Dev Biol* 123:411–420.
- Loreda GA, Brukman A, Harris MP, Kagle D, Leclair E, Gutman R, Denney E, Henkelman E, Murray BP, Fallon JF, Tuan RS, Gilbert SF. 2001. Development of an evolutionarily novel structure: fibroblast growth factor expression in the carapacial ridge of turtle embryos. *J Exp Zool* 291:274–281.
- Mannen H, Li SL. 1999. Molecular evidence for a clade of turtles. *Mol Phylogenet Evol* 13:144–148.
- Monsoro-Burq AH, Le Douarin NM. 2000. Duality of molecular signaling involved in vertebral chondrogenesis. *Curr Top Dev Biol* 48:43–75.
- Murakami Y, Ogasawara M, Sugahara F, Hirano S, Satoh N, Kuratani S. 2001.

- Identification and expression of the lamprey *Pax6* gene: evolutionary origin of the segmented brain of vertebrates. *Development* 128:3521–3531.
- Newgreen DF, Scheel M, Kastner V. 1986. Morphogenesis of sclerotome and neural crest in avian embryos. In vivo and in vitro studies on the role of notochordal extracellular material. *Cell Tissue Res* 244:299–313.
- Nikovits W Jr, Cann GM, Huang R, Christ B, Stockdale FE. 2001. Patterning of fast and slow fibers within embryonic muscles is established independently of signals from the surrounding mesenchyme. *Development* 128:2537–2544.
- Nowicki JL, Takimoto R, Burke AC. 2003. The lateral somitic frontier: dorso-ventral aspects of antero-posterior regionalization in avian embryos. *Mech Dev* 120:227–240.
- O'Hare MJ. 1972. Differentiation of chick embryo somites in chorioallantoic culture. *J Embryol Exp Morphol* 27:215–228.
- Ordahl CP. 1993. Myogenic lineages within the developing somite. In: Bernfield M, editor. *Molecular basis of morphogenesis*. New York: John Wiley and Sons. p 165–176.
- Pardanaud L, Luton D, Prigent M, Bourcheix LM, Catala M, Dieterlen-Lievre F. 1996. Two distinct endothelial lineages in ontogeny, one of them related to hemopoiesis. *Development* 122:1363–1371.
- Pinot M. 1969. Etude expérimentale de la morphogenèse de la cage thoracique chez l'embryon de poulet: mécanismes et origine du matériel. *J Embryol Exp Morphol* 21:149–164.
- Platz JE, Conlon JM. 1997. Reptile relationships turn turtle. . . and turn back again. *Nature* 389:246.
- Rieppel O. 2001. Turtles as hopeful monsters. *Bioessays* 23:987–991.
- Ruckes H. 1929. Studies in chelonian osteology part II, The morphological relationships between the girdles, ribs and carapace. *Ann N Y Acad Sci* 31:81–120.
- Sanders EJ, Prasad S, Cheung E. 1988. Extracellular matrix synthesis is required for the movement of sclerotome and neural crest cells on collagen. *Differentiation* 39:34–41.
- Schneider RA, Helms JA. 2003. The cellular and molecular origins of beak morphology. *Science* 299:565–568.
- Seno T. 1961. An experimental study on the formation of the body wall in the chick. *Acta Anat* 45:60–82.
- Serra JA. 1946. Histochemical tests for protein and amino acids: the characterization of basic proteins. *Stain Technol* 21:5–18.
- Sweeney RM, Watterson RL. 1969. Rib development in chick embryos analyzed by means of tantalum foil blocks. *Am J Anat* 126:127–150.
- Tokita M, Kuratani S. 2001. Normal embryonic stages of the Chinese softshelled turtle *Pelodiscus sinensis*. *Zool Sci* 18:705–715.
- Vincent C, Bontoux M, Le Douarin NM, Pieau C, Monsoro-Burq AH. 2003. *Msx* genes are expressed in the carapacial ridge of turtle shell: a study of the European pond turtle, *Emys orbicularis*. *Dev Genes Evol* 213:464–469.
- Walker WF Jr. 1947. The development of the shoulder region of the turtle, *Chrysemys picta marginata*, with special reference to the primary musculature. *J Morphol* 80:195–249.
- Watterson RL, Fowler I, Fowler BJ. 1954. The role of the neural tube and notochord in development of the axial skeleton of the chick. *Am J Anat* 95:337–399.
- Williams LW. 1910. The somites of the chick. *Am J Anat* 11:55–100.
- Williams JL. 1942. The development of cervical vertebrae in the chick under normal and experimental conditions. *Am J Anat* 71:153–175.
- Wilting J, Brand-Saberi B, Huang R, Zhi Q, Kontges G, Ordahl CP, Christ B. 1995. Angiogenic potential of the avian somite. *Dev Dyn* 202:165–171.
- Yntema CL. 1970. Extirpation experiments on the embryonic rudiments of the carapace of *Chelydra serpentina*. *J Morphol* 132:235–244.
- Zardoya R, Meyer A. 1998. Complete mitochondrial genome suggests diapsid affinities of turtles. *Proc Natl Acad Sci U S A* 95:14226–14231.
- Zardoya R, Meyer A. 2001a. On the origin of and phylogenetic relationships among living amphibians. *Proc Natl Acad Sci U S A* 98:7380–7383.
- Zardoya R, Meyer A. 2001b. The evolutionary position of turtles revised. *Naturwissenschaften* 88:193–200.